J. Ind. Geophys. Union (July 2011)
Vol.15, No.3, pp.161-170

Estimating the Viscosity of Rock Bodies - A Comparison Between the Hormuz- and the Namakdan Salt Diapirs in the Persian Gulf, and the Tso Morari Gneiss Dome in the Himalaya

Soumyajit Mukherjee
Department of Earth Sciences, Indian Institute of Technology Bombay, Powai, Mumbai- 400 076
E.mail: soumyajitm@gmail.com

ABSTRACT
Based on known extrusion rates, the viscosities of the Hormuz and the Namakdan salt diapirs in the Persian Gulf were estimated to be between 1.15×10^{17} and 8.75×10^{20} Pa s, and the Tso Morari gneiss dome in the Himalaya to be $\leq 10^{22}$ Pa s. The idea behind doing these exercises was that the deduced parameters would help us in building scaled analogue model of tectonics of these areas. Neglecting any gravity spreading, erosion and the geothermal gradient, these diapirs and domes were assumed to be incompressible Newtonian viscous fluids, which extruded at rates of few mm per year through channels of uniform elliptical or circular cross-sections driven by buoyant push arising from minor difference in density of the rocks at the bottom. However, while the salt diapirs rose $\leq$ 10 km through vertical channels for 10^4 yrs, the gneiss dome extruded hundreds or even thousands of km along a channel that plunged between 7^0 and 62^0 (maximum variation allowed by previous workers in their models) for 53 Ma covering hundreds or even thousands of km along the channel. Starting from the Poisson equation, the velocity profile of the salt diapirs are deduced to be time dependent and free from any overburden rocks, whereas that the velocity profile for the Tso Morari dome was independent to time and a plug of multi-lithology tried to prevent its extrusion were considered.

INTRODUCTION

That a body of fluid of higher density will sink in a surrounding immiscible fluid of lower density and displace it upward is a well known corollary of Archimedes' principle in fluid mechanics and is one of the mechanisms that drive isostasy. The most majestic manifestations of this physical process are the downbuilding of salt diapirs over last thousands of years from a shallow crustal depth up to a rates of 3 mm yr^{-1} (e.g. Koyi 1997), and bodies of ultra-high pressure metamorphic rocks that rise > 100 km equally fast from the asthenosphere–over several million years (Gulliot et al., 2009). One of the most fruitful applications of the concept of isostasy has been indirect estimations of the viscosities of the Earth's crust based on crustal rebound rates- the Fennoscandian shield being the classical study area (Schubert, Turcotte & Olson 2001). Recently Mukherjee, Talbot & Koyi (2010) estimated the viscosity of salts in the Hormuz and the Namakdan salt diapirs in the Persian Gulf (Fig.1) to range between 1.15×10^{17}-8.75×10^{20} Pa s. Mukherjee & Mulchrone (submitted) performed a sequel exercise on the Tso Morari gneiss dome in the western Indian Himalaya (Fig.2) and constrained its viscosity during extrusion to have been $\leq 10^{22}$ Pa s. This work aims *(i)* to compare the tectonic scenarios of these two very different study areas and summarize the findings of viscosity through analytical model, and *(ii)* explain the underlying extrusion principles. The study does not involve generation of any new geochemical data. Rather it uses the existing data to deduce the flow parameter.

The Salt Diapirs & the Gneiss Dome

The Neoproterozoic Cambrian salts of the Hormuz and the Namakdan diapirs in the Persian Gulf rose most of their way to the surface due to a Rayleigh-Taylor instability created by the downbuilding of superjacent Phanerozoic limestones of higher density (Fig.3). The salt also contains relatively small bodies of Paleozoic silicic igneous rocks. The local rise rates

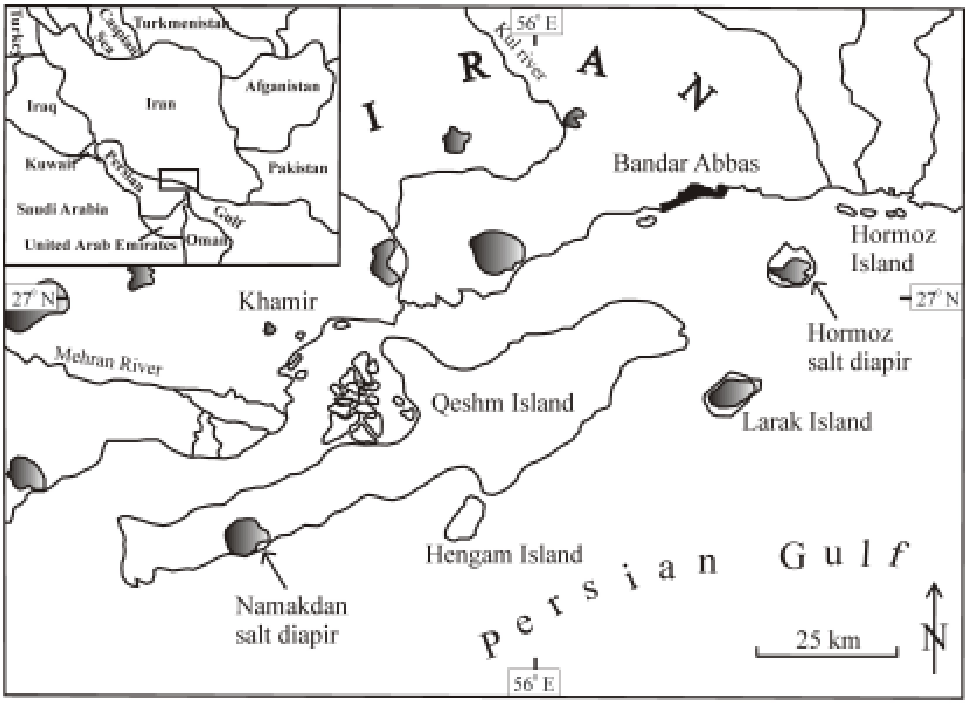

Figure 1. Geography of the Hormuz- and the Namakdan diapirs. Shaded areas represent exposed salts. Reproduced from Bruthans et al. (2006).

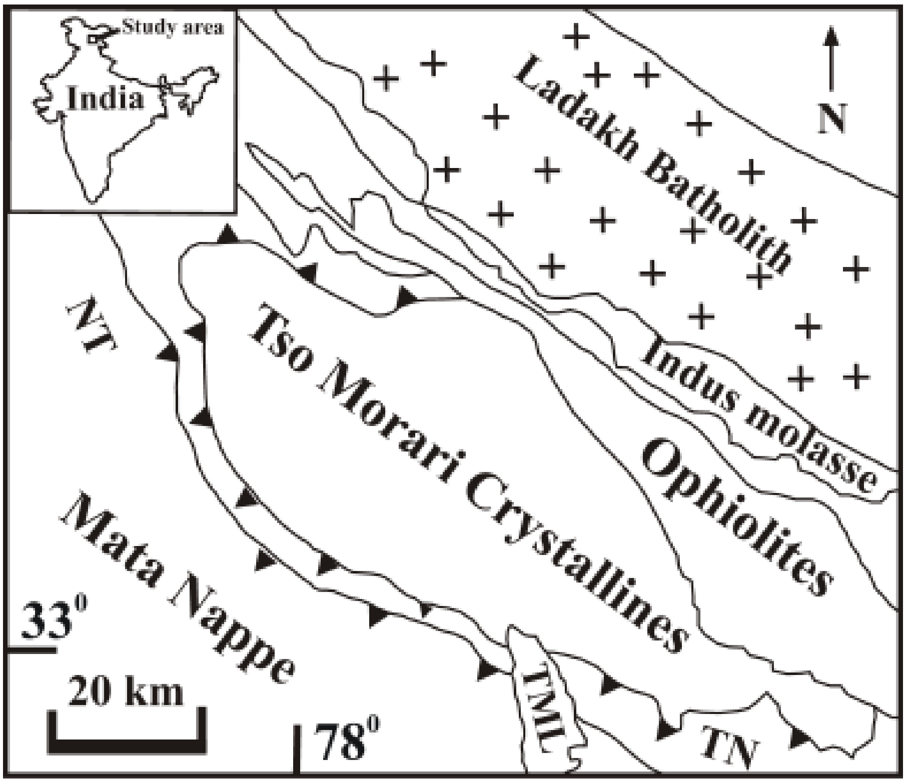

Figure 2. Geological map of the Tso Morari dome (reproduced partially from fig. 1 of Epard & Steck, 2008, but the term 'Tso Morari Nappe' of the authors is replaced with 'Tso Morari Dome' following Mukherjee & Mulchrone (submitted). TN- Tetraogal Nappe; NT- Nyimaling Thrust, TML- Tso Morari lake.

of these diapirs were found to match with that expected from a Newtonian fluid (Bruthans et al., 2006). The Proterozoic to Paleozoic qurtzofeldspathic Tso Morari orthogneiss rarely with some pelitic component, on the other hand, extruded as a NW-SE trending dome starting from ~ 53 Ma and from a depth of ~ 120 km through an inclined subduction channel located at the continental suture of the Indian- and the Eurasian plates (Mukherjee, Sachan & Ahmad 2005; also see Guillot et al., 2008) (Figs.4a,b). Recently the Dalhousie school modeled its extrusion as the ascent of an incompressible Newtonian viscous fluid (e.g. Beaumont et al., 2009). In such considerations, the properties of solids, such as the Poisson ratio, do not come into consideration. Ductile shear sense indicators indicative of their extrusion are not exposed on the flanks of the Hormuz and the Namakdan salt diapirs. However, the flank of the Tso Morari dome has revealed prominent mylonitization and extensional down-dip prominent ductile shear (Guillot, Hattori & Sigoyer 2000). The Hormuz and the Namakdan salt diapirs are still partially capped by recent marine sediments. On the other hand, the lithology of greywacke and carbonates that overlay TMC gneiss now surrounds its flank (Epard & Steck 2008).

As expected in natural cases, both the salts in the Hormuz and the Namakdan diapirs, and the gneiss in the Tso Morari dome are 'impure'. For example, both thee salt diapirs include < 1% by volume of mélange of inclusions' of sedimentary (sandstone, limestone, dolostone, shale, siltstone), igneous (rhyolite, andesite, ignimbrite, trachyte, granite, gabbroic rocks, metaphyres, tuffs) and metamorphic rocks (schists, gneisses, metabasites, quartzite) (Bruthans et al., 2006; and references therein). In the TMC gneiss, on the other hand, there are reports of much smaller amounts of serpentinites (in the mélange part), carbonates and eclogites (Sachan, Mukherjee & Ahmad 2005 but also others). This is one more reason why taking a range of density values of the lithologies are justified in the extrusion models of Mukherjee, Talbot & Koyi (2010) and Mukherjee & Mulchrone (submitted) rather than single specific values.

The shapes of the channel through which the salt and the gneiss flowed were similar, i.e. a cylinder with a uniform elliptical cross-section. However, the lengths, areas and plunges of these channels were drastically different (compare Figs.3 and 4). For example, *(i)* the length of the channel in the Hormuz and the Namakdan diapirs are much shorter (d" 10 km; Koop & Stonely 1982; Bahroudi & Talbot 2003) than the ~ 120 km (Mukherjee, Sachan & Ahmad 2005; Guillot et al., 2008) for the Tso Morari dome. *(ii)* In cross-sections, the two salt diapirs have very low ellipticity (= major axis divided by the minor

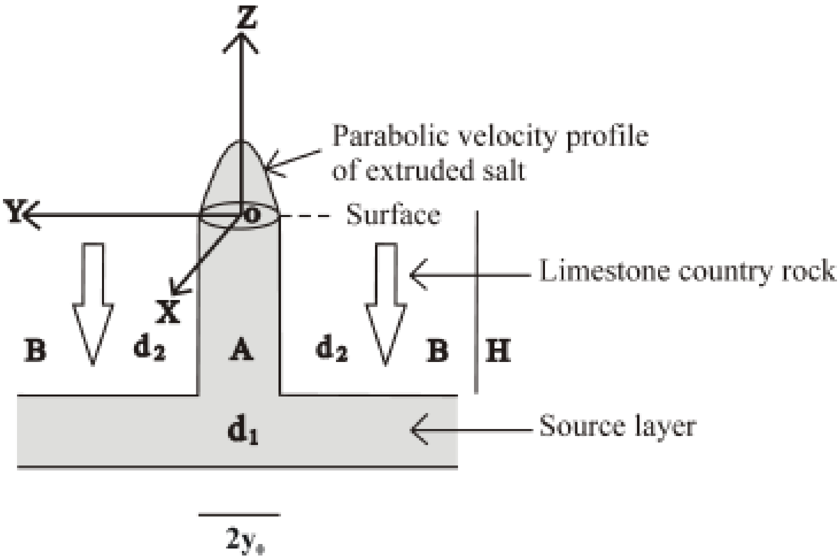

Figure 3. Mechanical model of salt extrusion. A: vertical column with an elliptical cross-section for the Hormuz diapir and a circular one for the Namakdan diapir of diameter '$2y_0$' units. 'A' is of length 'H' and is connected with a horizontal channel. Both the channels are full of salts of density d_1. Overburden limestones of density d_2 (> d_1) exerts pressure and extrudes salts through 'A'. Reproduced from Mukherjee, Talbot & Koyi (2010).

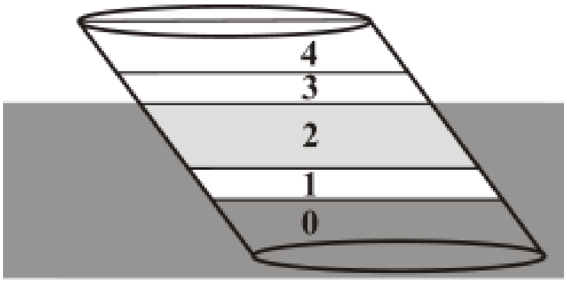

Fig. 4a

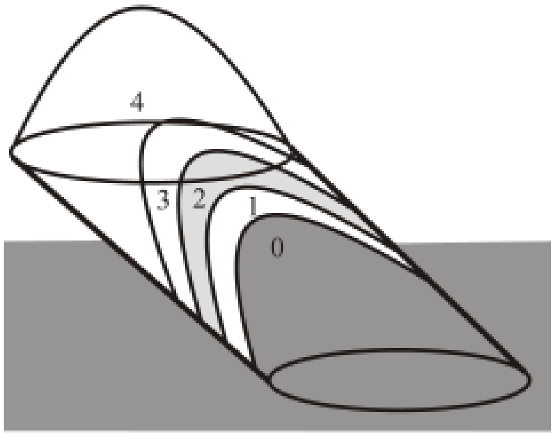

Fig. 4b

Figure 4. Disposition of lithologies in the inclined channel before (Fig. 4a) and during (Fig. 4b) extrusion. The two shaded layers represent mantle that may have different densities. Layer-0: mantle; layer-1: proto-TMC gneiss; layer-2: mantle; layer-3: crust of known lithology; layer-4: crust of unknown lithology. Neither to scale nor angle. Reproduced from Mukherjee & Mulchrone (submitted).

axis) of e ~1.3 (Bruthans et al., 2006; Mukherjee, Talbot & Koyi 2010). By contrast, the Tso Morari dome outcrop is an irregular ellipse (Fig. 1 of Epard & Steck 2008). Mukherjee & Mulchrone (submitted) obtained a best fit ellipse (Fig.5) on this outcrop and deduced the lengths and trends of its major- (90 km, SE-NW) and the minor axis (32 km, NE-SW) and a high ellipticity of 2.81. Physical boundary conditions of the diapirs and the dome are presented between columns 7 to 11 in Table-1.

The densities of the extruding rocks and their overburdens in the diapirs and the dome are unknown. The widest possible variations of these values were, therefore, collected from literature (columns 4, 14 and 16 in Table 1). These data were used in the extrusion models of Mukherjee, Talbot & Koyi (2010) and Mukherjee & Mulchrone (submitted) to calculate a range of viscosities (the last column in Table 1; also see Fig. 6 and its caption). The two salt diapirs were extruded by the sinking of limestone 0.17 to 0.8 gm cm^{-3} more dense than the salts. On the other hand, the extrusion of the TMC was driven by sinking of a mantle layer with a similar density difference that ranged from 0.22 to 0.81 gm cm^{-3}.

The extrusion rates of the salts in the two diapirs and the gneiss in the TMC dome was mostly of the order of few mm per year. Detailed geochronologic studies by Epard & Steck (2008) demonstrated a fall in extrusion rate of the TMC gneiss dome- in the last 30 Ma the rate was 0.5 mm yr^{-1}. However, Bruthans et al., (2006) was not sure of any change in extrusion rate of the salt diapirs. The data set of extrusion rates at particular locations of the Hormuz and the Namakdan diapirs come all from Bruthans et al., (2006). Those for the Tso Morari Gneiss dome come from Guillot, Hattori & Sigoyer (2000); de Sigoyer, Guillot & Dick (2004); Sachan, Mukherjee & Ahmad (2005); and Epard & Steck (2008). The extrusion rates of these diapirs and the dome are

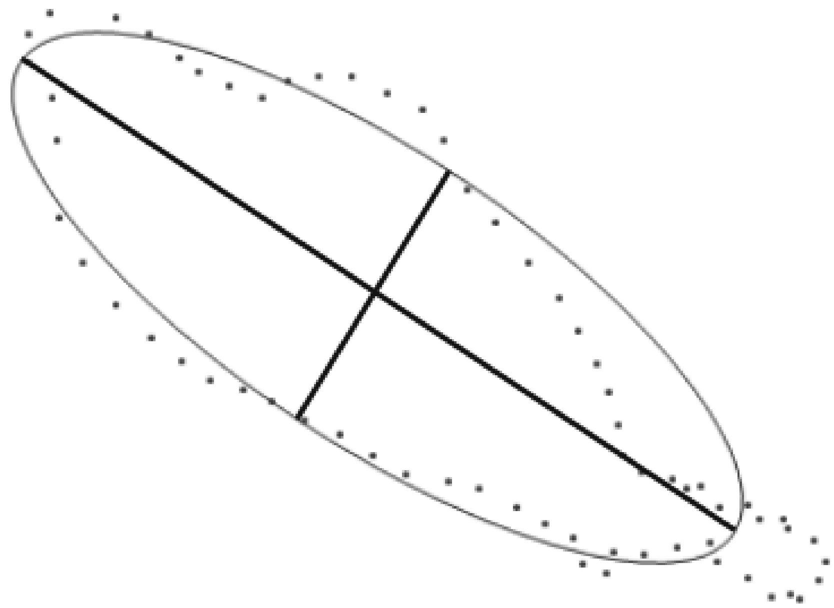

Figure 5. Considering sixty six points on its margin, the sub-elliptical outcrop of the Tso Morari dome was approximated with a best fit ellipse (reproduced from Mukherjee & Mulchrone submitted).

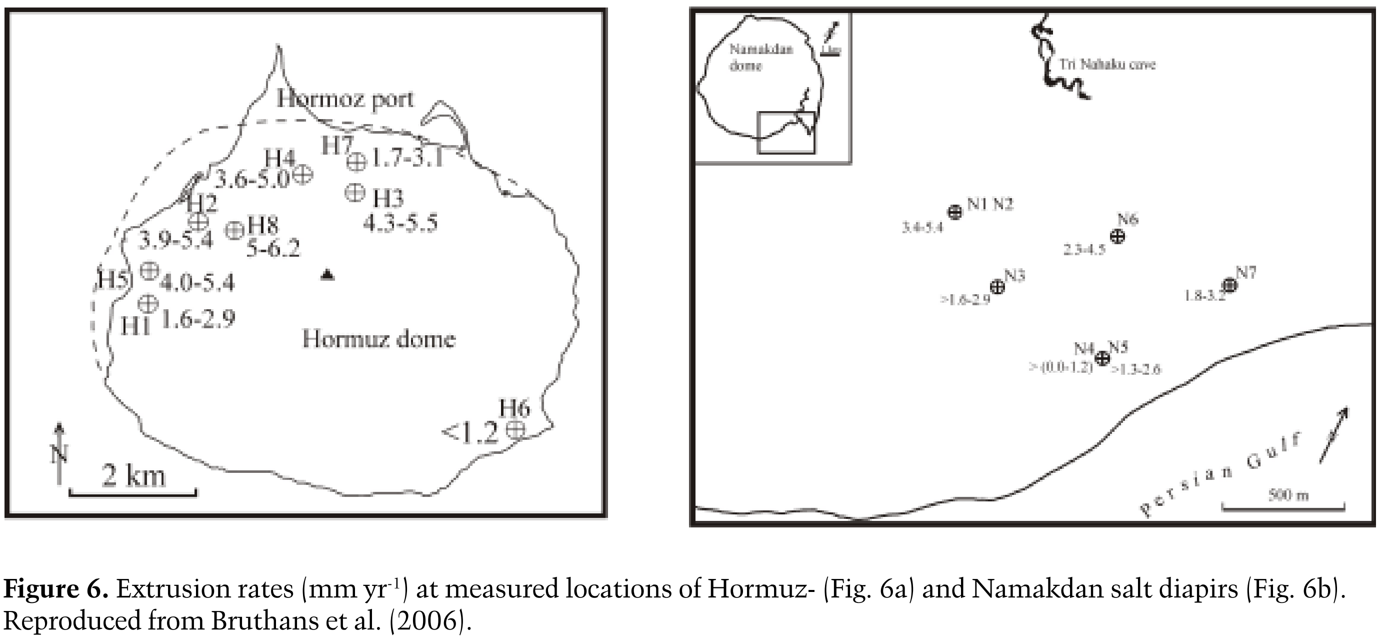

Figure 6. Extrusion rates (mm yr^{-1}) at measured locations of Hormuz- (Fig. 6a) and Namakdan salt diapirs (Fig. 6b). Reproduced from Bruthans et al. (2006).

listed in the sixth column of Table-1. The TMC gneiss extruded from ~ 120 km depth through a channel that plunged at angles ranging from 7 to 62^0. Taking these two limiting values of the plunge, allows an estimate of the distance that the TMC gneiss moved along the channel to between ~ 234.4 and 1698.5 km. By contrast, the Hormuz and the Namakdan salt bodies traveled ≤ 10 km (Mukherjee, Talbot & Koyi 2010). While the time taken by the TMC gneiss to reach the surface was 53 Ma (Epard & Steck 2008), that for the Hormuz and the Namakdan diapirs were only 10^4 yrs.

Table 1. Physical boundary conditions, flow parameters and the estimated viscosities in Mukherjee, Talbot & Koyi (2010) for the salt domes, and Mukherjee & Mulchrone (submitted) for the TMC gneiss dome.

	Extruding material					Channel shape, size and orientation					Overburden			Material that gave buoyant push		Extruding material
Study area	Rock type	Vertical thickness (km) before extrusion	Density (gm cm^{-3})	Time (yrs) taken to extrude	Extrusion rates (mm yr^{-1})	Dip (in degrees)	Length (km)	Major axis (km)	Minor axis (km)	Elliptic-ity	Lithology	Thick-ness (km)	Density (gm cm^{-3})	Lithology	Density (gm cm^{-3})	Estimated viscosity (Pa s)
Hormuz dome	Impure salt	Uncons-trained	2-2.2	10^4	5, 4.27, 2.5, 5.7, 4.7, 2,2, 4.7	90	10	8.5	6.8	1.25	-	-	-	Limestone	2.37-2.8	10^{18}-10^{21}
Namakdan dome	Impure salt	Uncons-trained	2-2.2	10^4	4.7, 4.1, 2.55, 2.45, 3.75, 3	90	8	7	6.8	1.03	-	-	-	Limestone	2.37-2.8	10^{17}-10^{21}
Tso Morari dome	Impure gneiss	7	2.59-3.12	53×10^6	7, 0.25, 0.5, 1, 1.2, 30, 5	7, 62	226.53	90	32	2.81	Mantle	16.8, 41.8	2.9-3.4	Mantle	2.9-3.4	$\leqslant 10^{22}$
											Turbidites, ophiolites	8.2	2.62-3.69			
											Crust of unknown lithology	25-50	2.7-2.9			

MODELS & RESULTS

The starting equation in estimating the viscosities is the well known 'Poisson equation':

$$(\partial^2U_z/\partial x^2)+(\partial^2U_z/\partial y^2)=\mu^{-1}[(\partial P/\partial z)-d_1 g\mathrm{Sin}\theta] \qquad (1)$$

The use of this equation is to build up an extrusion model of the domes in different contexts. The equation (same as eqn 6.190 of Papanastasiou, Georgiou & Alexandrou 2000) considers the laminar flow of an incompressible Newtonian viscous fluid due to a pressure gradient '$\partial P/\partial z$'. The fluid has a density 'd_1' and a velocity 'U_z' takes place against gravity along the 'Z' direction through an infinitely long channel that dip at an angle of 'θ'. 'X' and 'Y' are the axes on the cross-section of the channel. In the present cases of salt diapirs, sinking of a fluid of density 'd_2' (> d_1) pushes the low density fluid through a vertical ($\theta = 90^0$) channel (Fig.3), so that:

$$(\partial^2Uz/\partial x^2)+(\partial^2Uz/\partial y^2)=\mu^{-1}[g\ (d_2-d_1)-P_{out}(t)\ H^{-1}] \qquad (2)$$

where $P_{out}(t)$ is the pressure exerted by the temporally piling up of the extruded fluid above the vent.

Mukherjee, Talbot & Koyi (2010) derived the solution of this equation is as follows:

$$U_z\ (x,y,t) = 0.5g\ \mu^{-1}\ a^2\ b^2\ (d_2-d_1)\ (a^2 + b^2)^{-1} \times (1-x^2\ a^{-2} - y^2\ b^{-2})\ (1 - t\ \tau^{-1}) \qquad (3)$$

where $\tau = [4\ \mu\ H\ a^{-2}\ b^{-2}\ d^{-1}\ 1\ g^{-1}\ (a^2 + b^2)]$ (4)

In a simplified case of a circular cross-section of radius 'y_0', i.e. $a = b = y_0$, eqn (3) simplifies to $U_z\ (y_1,t) = 0.25\ g\ \mu^{-1}\ (d_2 - d_1)\ (y_0^2-y_1^2)\ (1-t\ \tau^{-1})$ (5) and eqn (5) to $\tau = 8\ \mu\ H\ y_0^{-2}\ d^{-1}\ g^{-1}$ (6)

The velocity profile given by eqn (3) is dependent on time (t). However, if the effect of the pressure exerted by the up-building fluid is neglected, i.e. $P_{out}(t) = 0$, eqn (2) takes the following form when a channel with 'θ' plunge is considered (Mukherjee & Mulchrone, submitted) (Fig. 4a), which is independent of 't':

$$U_z\ (x,y) = 0.5g\ \mu^{-1}\ a^2\ b^2\ \mathrm{Sin}\theta\ (d_2 - d_1)\ (a^2 + b^2)^{-1} \times (1 - x^2\ a^{-2} - y^2\ b^{-2}) \qquad (7)$$

At the centre ($x = y = 0$), $0.5g\ \mu^{-1}\ a^2\ b^2\ \mathrm{Sin}\theta\ (d_2 - d_1)\ (a^2 + b^2)^{-1}$ (8)

When an overburden of three immiscible layers of fluids with their lengths along the channel 'h_2', 'h_3' and 'h_4' (Fig. 4a) and densities 'd_2', 'd_3' and 'd_4' at the top of the fluid column of density 'd_1' is considered, eqn (7) takes the following form

$$U_z\ (0,0) = 0.5\ \mu^{-1}\ g\ a^2\ b^2\ \mathrm{Sin}\theta\ (d - d_1\ h_1\ H^{-1}-d_2\ h_2\ H^{-1}-d_3\ h_3\ H^{-1}-d_4\ h_4\ H^{-1})(a^2 + b^2)^{-1} \qquad (9)$$

While Mukherjee, Talbot & Koyi (2010) used eqn (4) to put extrusion rates at known coordinates and calculate the viscosity of the Hormuz diapir considering it to have a perfectly elliptic section, and eqn (5) for the Namakdan diapir considering its section to be circular; Mukherjee & Mulchrone (submitted) used eqn (9) to put extrusion rates at the model center of the ellipse of best fit on the sub-elliptical profile of the subduction channel through which the TMC gneiss rose. The locations of known extrusion rates for the two salt diapirs are shown in Figs. 6a and -b. The set of chosen parameters for which the optimum values of viscosities are deduced for the diapirs and the dome are presented in Tables 2 to 4. The east and the north directions for the Hormuz diapir were considered to be that of the positive directions of the X and the Y-axis. Thus, coordinates of points lying at the west (or south) of the centre of the diapir were taken negative (e.g. the data for the second column at the second row in Table 2). The three layers of overburdens considered from top to bottom are: the crust of unknown lithology, a crustal layer of known lithology (mainly turbidites and ophiolites) and a mantle layer (see column 12 of Table 1). The former layers now flank of the TMC gneiss dome as the Tetraogal Nappe, the Mata Series of rocks, and the Karzok Ophiolite Complex.

Mukherjee, Talbot & Koyi (2010) estimated the viscosity of the Hormuz diapir to be 10^{18} -10^{21} Pa s, and 10^{17} -10^{21} Pa s for the Namakdan diapir. Reviewing 37 viscosity values of salts in the literatures since 1967, they concluded that their viscosity estimates were higher than usually taken for natural salts but the data matched with other salt diapirs. Mukherjee & Mulchrone (submitted), on the other hand, estimated the maximum viscosity of the TMC gneiss to be $\leq 8\times 10^{22}$ Pa s. Compared to previous data on viscosity, summarized here in Table 5, they concluded that the TMC gneiss could be 10^2 order of magnitude more sluggish than other gneisses and granites, although the estimated maximum limit broadly conformed with that for crustal channels and lithospheric and asthenospheric values. Notice that while Mukherjee, Talbot & Koyi (2010) gave a range of viscosity values for salts, Mukherjee & Mulchrone (submitted) could produce only the upper limit of viscosity of the gneiss. This was because, unlike Mukherjee, Talbot & Koyi (2010) who input only the boundary values of densities in eqn (2), Mukherjee & Mulchrone (submitted) considered all possible values of densities and in their respective ranges in eqn (6), which led in some cases ($d - d_1 h_1 H^{-1} - d_2 h_2 H^{-1} - d_3 h_3 H^{-1} - d_4 h_4 H^{-1}$) to be < 0 leading to hypothetical negative values of viscosities indicative

Table 2. Calculation of a range of viscosity 1×10^{18} to 8.75×10^{20} Pa s, shown in bold in table, for the Hormuz dome. It is a partial reproduction of table 1 of Mukherjee, Talbot & Koyi (2010). Eqns (3) and (4) were utilized. See Fig. 6a for sample locations.

Sample number	'x' coordinate in km	'y' coordinate in km	Extrusion rate U_Z (x,y,t) (in mm yr^{-1})	μ_{max} (in Pa s), for $d_{max\,diff}$ = 0.8 gm cm^{-3}	μ_{min} (in Pa s), for $d_{min\,diff}$ = 0.17 gm cm^{-3}
H_3	+ 0.39	+ 1.17	5.00	1.29×10^{20} **1×10^{18}**	2.67×10^{19} 1.1×10^{18}
H_2	-1.83	0.83	4.7	**8.75×10^{20}** **1×10^{18}**	1.85×10^{20} 1.03×10^{18}

Table 3. Calculation of a range of viscosity 1.15×10^{17} to 6.5×10^{20} Pa s, shown in bold in table, for the Namakdan dome. Eqns (5) and (6) were utilized. It is a partial reproduction of table 2 of Mukherjee, Talbot & Koyi (2010). See Fig. 6b for sample locations.

Sample Number	Distance from centre (km)	Extrusion rate U_Z (y_1,t) (in mm yr^{-1})	μ_{max} (in Pa s), for $d_{max\,diff}$ = 0.8 gm cm^{-3}; 2 y_0 = 7 km	μ_{min} (in Pa s), for $d_{max\,diff}$ = 0.17 gm cm^{-3}, 2 y_0 = 7 km	μ_{max} (in Pa s), for $d_{max\,diff}$ = 0.8 gm cm^{-3}; 2 y_0 = 6.8 km	μ_{min} (in Pa s), for $d_{max\,diff}$ = 0.17 gm cm^{-3}, 2 y_0 = 6.8 km
$N_{1/2}$	2.25	4.7	8.9×10^{19} 1.2×10^{18}	1.99×10^{20} 1.5×10^{18}	7.39×10^{19} **1.15×10^{17}**	1.67×10^{20} 3.3×10^{19}
N_{7A}	3.31	2.55	3.1×10^{19} 1.2×10^{18}	**6.5×10^{20}** 2.95×10^{18}	1.38×10^{20} 1.2×10^{18}	No real solution No real solution

Table 4. Calculation of maximum possible viscosity of 10^{22} Pa s of the Tso Morari gneiss. 'd_1', 'd_2', 'd_3', 'd_4' (in gm cm^{-3}): 2.59-3.12, 2.9-3.4, 2.22-2.90, 2.7-2.9, respectively. 'd_1' to 'd_4' correspond to densities of layers of lengths 'h_1' to 'h_4'. 'd' of the bottommost layer ranges between 2.9-3.4 gm cm^{-3}. Eqn (9) is utilized in this calculation. It is a partial reproduction of table 1 of Mukherjee & Mulchrone (submitted).

Channel dip (in degrees)	h_1 (km)	h_2 (km)	h_3 (km)	h_4 (km)	H (km)	μ_{max} (in Pa s),
7	57.4	1162.7	68.1	410.3	1698.5	10^{22}

Table 5. Relevant viscosities compiles by Mukherjee & Mulchrone (submitted) is reproduced to compare with that estimated for the TMC gneiss.

Lithology	Viscosity (in Pa s)
Granites at 700 ^{0}C	10^5-10^{12}
Granites at 1400 ^{0}C	2×10^5
Granite at near surface condition	~ 10^{20}
Asthenosphere in average	10^{19} - 10^{21}
Asthenosphere in the Indian - Eurasia collision zone	5×10^{18}
Lithosphere	10^{21} - 10^{23}
Crustal channel	6×10^{18}
Strong mantle lithosphere	10^{22} - 10^{24}
Weak mantle lithosphere	10^{19} - 10^{20}
Lowe crust below Tibet	6×10^{18}

of unrealistic combinations of flow parameters. Thus the lower limit of viscosity of the TMC gneiss remained unconstrained.

COMPARISON

The underlying mechanism of extrusion considered in Mukherjee, Talbot & Koyi (2010) and in Mukherjee & Mulchrone (submitted) are the followings. *(i)* The rock/geological body was considered to be a Newtonian viscous fluid. Such fluids obey the simple relation of proportionality between the applied stress and the strain rate. While this assumption is justified for the two salt diapirs since Bruthans et al., (2006) had already established this point, it was certainly a simplified consideration for the TMC gneiss. The reason is that Treagus & Sokoutis (1992) compiled various magnitudes of *stress exponent* (n), varying from 3 to 6 or more, in shear zones in the following constitutive equation:

$$(d\varepsilon/dt) = A\ \sigma^n \qquad (10)$$

where '$d\varepsilon/dt$' is the steady state strain rate on a fluid, 'σ' is the differential stress, 'A' is a material constant, and 'n' is the stress exponent. For n = 1, the fluid is Newtonian. However, the stress exponent specifically for the TMC gneiss is unknown but since it extruded from a depth of > 100 km, i.e. certainly from the asthenosphere, the flow exponent (n) could be 4 ± 1 (Melson 1980; also see Polyansky et al., 2010). In the present study, however, I followed the simple assumption of Newtonian rheology as done by Whitney, Teyssier & Vanderhaeghe (2004). *(ii)* Further, the two materials- salts and the gneiss were considered incompressible. Salt is practically incompressible over a wide range of temperature and pressure (Hudec & Jackson 2007). The kinematic dilatancy of the salt diapirs and the gneiss dome has not yet been established. *(iii)* Erosion of the extruded materials was neglected both in cases of Mukherjee, Talbot & Koyi (2010) as well as Mukherjee & Mulchrone (submitted). The key reason is that although erosion prevailed during extrusion, it was not focused specifically over those diapirs and the dome. *(iv)* Geothermal gradient was neglected in both cases. The rationales are- while the subduction channel through which the Tso Morari Gneiss rose had quite a low geothermal gradient presumably of < 10 ^{0}C km^{-1} (Guillot et al., 2009); the salt diapirs were presumably subject to a normal geothermal gradient of 30 ^{0}C km^{-1} (Khutorskoi et al., 2010) down to the mother layer of salt at merely ~ 10 km can give a maximum temperature variation of just ~ 300 ^{0}C. *(v)* Lateral gravitational spreading was neglected in both the salt and the gneiss domes. Mukherjee & Mulchrone (submitted) considered that the rock overburden to the TMC gneiss shielded the former spreading for a considerable time span. On the other hand, the parabolic velocity profiles of the salt diapirs deduced by Bruthans et al., (2006) was considered by Mukherjee, Talbot & Koyi (2010) indicative of their insignificant spreading.

The final fluid mechanical equations on which Mukherjee , Talbot & Koyi (2010) and Mukherjee & Mulchrone (submitted) worked are different in the following ways. *(i)* The fluid mechanical derivation by Mukherjee & Mulchrone (submitted) took care of the hindrance created by the mass of the overburden plug that tried to resist the extrusion of the TMC gneiss. However, Mukherjee, Talbot & Koyi (2010) did not consider any overburden above the salt column. *(ii)* Instead, they took account the mass of the extruded salt as hindering further extrusion by reducing the pressure gradient that drove the salt. In contrast, Mukherjee & Mulchrone (submitted) did not consider any role of progressively piled up overburden.

CONCLUSIONS

This paper compares two studies, Mukherjee , Talbot & Koyi (2010) and Mukherjee & Mulchrone (submitted), on indirect estimation of viscosity of geological bodies based on approach applied to the crustal rebound rates. In one of the study areas in the Persian Gulf, the post Miocene rise of the Hormuz and the Namakdan salt diapirs took place due to a Rayleigh-Taylor instability because higher density limestones overlies its source layer. In the second study area in the Himalaya, the Tso Morari gneiss extruded through a subduction channel at the leading edge of the Indian continental crust. The estimated viscosity ranges for the salt diapirs were 1.15×10^{17} to 8.75×10^{20} Pa s, and $\leq 10^{22}$ Pa s for the Tso Morari gneiss. Impurities in lithology in these diapirs and the dome justify assigning ranges of viscosity values rather than specific magnitudes. The estimated values for the salts matched those available from other salt diapirs in the world, and that for the gneiss dome matched viscosities previous constrained for the crustal channel, the lithosphere and the asthenosphere.

The common approach in these works have been that *(i)* the geological bodies were considered to be Newtonian viscous. While this is a concrete assumption for the studied salt diapirs, for the Himalayan gneiss it is only tentative. (ii) The bodies were further assumed to be incompressible. *(iii)* Those diapirs extruded through a very long smooth channel with uniform elliptical (or circular) cross-section. *(iv)* Extrusion took place due to sinking of denser limestone in the salt diapirs, and mantle in the gneiss dome. *(v)* A density difference from 0.17 to 0.81 gm cm^{-3} between the extruding diapirs and the dome and the sinking surroundings led to extrusion rates of a few mm per year. *(vi)* Gravitational spreading, erosion and the geothermal gradients are neglected in all cases for geologic reasons.

Although viscosity estimation of the salt diapirs and the Himalayan gneissic domes are based on the Poisson equation, the following dissimilarities exist between their physical boundary conditions *(i)* While the UHP rock extruded from a depth of 120 km, the salt diapirs rose only few km. *(ii)* The salt diapirs extruded through vertical channels (stems); whereas the TMC gneiss extruded through a gently (7^0) or a steeply dipping (62^0) channel. *(iii)* Thus while the salt diapirs traveled no more than 10 km, the Himalayan gneiss moved a very long distance of 226.53 to 1640.69 km. *(iv)* The extrusion rates in both cases was a few mm per year, the Himalayan gneiss took a very long span of ~ 53 Ma to extrude, whereas only the last 10^4 yrs were considered for the salt diapirs. *(v)* While the studied salt diapirs are circular or sub-circular in cross-sections, the TMC dome is strongly elliptical. *(vi)* The salt extrusion was considered to take place without any overburden, whereas a three-layer plug hindered but could not prevent the latter extrusion. *(vii)* The weight of the extruded salt was considered to lower the effective pressure gradient of the salt diapirs, whereas this was not taken into account in the Himalayan gneiss dome.

ACKNOWLEDGEMENTS

IIT Bombay's flexible Seed Grant: Spons/GS/SM-1/ 2009. Chris Talbot (retired from Uppsala University) mentored and provided thorough comments that drastically improved both the English and the scientific contents. Dr. Barun Mukherjee (Wadia Institute of Himalayan Geology) made a thoughtful review. Dr. N. Venkateswarlu (NGRI) is thanked for his efficient and intense editorial work.

REFERENCES

Bahroudi, A. & Talbot, C. J., 2003. The configuration of the basement beneath the Zagros basin. J. Petroleum Geol., 26, 257–82.

Beaumont, C., Jamieson, R.A., Butler, J. P. & Warren, C.J., 2009. Crustal structure: A key constraint on the mechanism of ultra-high-pressure rock exhumation. Earth Planet. Sci. Lett., 287, 116-129.

Bruthans, J., Fillipi, M., Geršl, M., Zare, M., Melková, J., Pazdur, A. & Bosak, P., 2006. Holocene marine terraces on two salt diapirs in the Persian Gulf, Iran: age, depositional history and uplift rates. J. Quarter. Sci., 21, 843–57.

de Sigoyer, Guillot, G. & Dick, P., 2004. Exhumation of the ultrahigh pressure Tso Morari unit in eastern Ladakh (NW Himalaya): A case study. Tectonics, 23, TC3003.

Epard, J.L. & Steck, A., 2008. Structural development of the TsoMorari ultra-high pressure nappe of the Ladakh Himalaya. Tectonophysics, 451, 242–264.

Guillot, S., Hattori, K., Agard, P., Schwartz, S. & Vidal, O., 2009. Exhumation processes in Oceanic and Continental Subduction Contexts: A Review. In: Lallemand, S. and Funiciello, F. (Eds.), Subduction Zone Geodynamics. Springer-Verlag Berlin Heidelberg. pp. 175-205.

Guillot, S., Hattori, K. & Sigoyer, D., 2000. Mantle wedge serpentinization and exhumation of eclogites: Insights from eastern Ladakh, northwest Himalaya. Geology, 28, 199-202.

Guillot, S., Mahéo, G., de Sigoyer, J., Hattori, K.H & Pêcher, A., 2008. Tethyan and Indian subduction viewed from the Himalayan high- to ultrahigh-pressure metamorphic rocks. Tectonophysics, 451, 225-241.

Hudec, M.R. & Jackson, M.P.A., 2007. Terra Infirma: Understanding Salt Tectonics. Earth-Sci. Rev., 82, 1-28.

Khutorskoi, M.D., Teveleva, E.A., Tsybulya, L. A., Urban, G. I., 2010. Heat Flow in Salt-Dome Basins of Eurasia: A Comperative Study. Geotectonics, 44, 289-304.

Koop, W.J. & Stonely, R., 1982. Subsidence history of the Middle East Zagros basin, Permian to recent. Phil Trans Royal Soc, London, A305, 149–68.

Koyi, H.A., 1997. Analogue modelling: from a qualitative to a quantitative technique, a historical outline. J. Petroleum Geol., 20, 223–38.

Melson, H.J., 1980. Rheology of the Earth: Theory and Observation. North Holland Publishing Company. Amsterdam. In: Dziewonski, A. M. (ed) Proceedings of the International School of Physics. pp. 318-336.

Mukherjee, B., Sachan, H.K. & Ahmad, T., 2005. A new occurrence of microdiamond from Indus Suture zone, Himalata: a possible origin. In: Memoire, H.S. (Ed.), Special extended Abstract Volume. Géologie Alpine, vol. 44, p. 136

Mukherjee, S. & Mulchrone, K. (submitted) Estimating the Viscosity of the Tso Morari Gneiss Dome, western Indian Himalaya. Int. J. Earth Sci.

Mukherjee, S., Talbot, C.J. & Koyi, H. A., 2010. Estimating the Viscosities of two Salt Diapirs in the Persian Gulf: Hormoz & Namakdan. Geol. Mag., 147, 497-507.

Papanastasiou, C.T., Georgiou, G.C. & Alexandrou, A.N. 2000. Viscous Fuid Flow. Florida: CRC Press, 253 pp.

Polyansky, O.P., Babichev, A.V., Korobeynikov, S.N. & Reverdatto, V.V., 2010. Computer modeling of Granite Gneiss Diapirism in the Earth's Crust: Controlling Factors, Duration, and Temperature Regime. Petrology, 18, 432-446.

Sachan, H.K., Mukherjee, B.K. & Ahmad, T., 2005. Coldsubduction of the Indian continental crust: Evidence from Tso-morari region, Ladakh, India. Him. Geol., 26, 25-32.

Schubert, G., Turcotte, D.L. & Olson, P., 2001. Mantle Convection in the Earth and Planets. Part I. Cambridge University Press, 498 pp.

Treagus, S.H. &Sokoutis, D., 1992. Laboratory modelling of strain variation across rheological boundaries. J. Struct. Geol., 14, 405-424.

Whitney, D.L., Teyssier, C. & Vanderhaeghe, O., 2004. Gneiss domes and crustal flow. In: Whitney, D. L., Teyssier, C., Siddoway, C. S. (eds) Gneiss domes in Orogeny. Geol. Soc. Am. Sp. Pub., 380, 15-33.

(Revised accepted 2011 June 17, Received 2011 January 25)

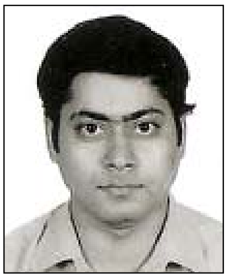

Dr.Soumyajit Mukherjeee (Assistant Professor, Department of Earth Sciences, Indian Institute of Technology Bombay) : Associate Editor for the 'International Journal of Earth Sciences'(Springer Publisher, Impact Factor : 2.445; formerly known as'Geologische Rundschau'). Fields of research : Ductile deformation, extrusion processes and their analytical models. Recepient of (i) 'Guest Scholarship' (Swedish Institute) to work in the 'Hans Ramberg Tectonic Lab' (Uppsala University) during 2005-2006 and (ii) 'Hutchison Young Scientist Award' from the 'International Union of Geological Sciences' (IUGS) in 2004.